IEEE Access
Multidisciplinary | Rapid Review | Open Access Journal

Received 4 February 2023, accepted 13 February 2023, date of publication 16 February 2023, date of current version 23 February 2023.

Digital Object Identifier 10.1109/ACCESS.2023.3246088

RESEARCH ARTICLE

Underfrequency Load Shedding Strategy With an Adaptive Variation Capability for Multi-Microgrids

RAN CHEN[1], HANPING XU[1], LI ZHOU[1], JIE CAI[1], CHUANYU XIONG[1], YINGBO ZHOU[1], XUEFEI ZHANG[2,3], QINGGUO DONG[4], CAN WANG[2,3], (Member, IEEE), AND NAN YANG[2,3], (Senior Member, IEEE)

[1]State Grid Hubei Economic Research Institute, Wuhan 430077, China
[2]Hubei Provincial Collaborative Innovation Center for New Energy Microgrid, China Three Gorges University, Yichang 443002, China
[3]College of Electrical Engineering and New Energy, China Three Gorges University, Yichang 443002, China
[4]State Grid Heze Power Supply Company, Heze, Shandong 274000, China

Corresponding author: Can Wang (xfcancan@163.com)

This work was supported by the Science and Technology Program of State Grid Hubei Electric Power Company Ltd., under Grant B31538221024.

ABSTRACT Multi-microgrids (MMGs) suffer from power shortages due to the loss of utility grid support when an unintentional transition occurs. This imposes a transient shock on the system voltage and frequency. To maintain the frequency stability and power balance of an islanded MMG, this paper presents an underfrequency load shedding (UFLS) strategy with adaptive variation. A comprehensive load evaluation method based on a composite least squares support vector machine (CLS-SVM) is proposed to ensure uninterrupted power for critical loads. This method considers the comprehensive evaluation influence factors (CEIFs) of loads. Then, a least squares support vector machine (LS-SVM) provides the load shedding determination factors, transforming the problem of determining critical loads into a 0-1 planning problem. A method with adaptive variation is proposed to solve the UFLS model. The effectiveness of the proposed strategy is verified for an MMG model based on a modified IEEE 33-bus system. The test results show that: 1) the average accuracy of the proposed method is 21.05% higher than that based on LS-SVM; 2) compared with UFLS strategies based on the load level alone and on an intelligent algorithm, the frequency fluctuation range of the proposed strategy is 12.50% and 19.23% lower, respectively, and the frequency recovery time is 3.90% and 5.73% shorter, respectively; 3) compared with PSO, GOA and GA, the standard deviation of the iterative mean of the proposed algorithm decreases by 36.22%, 53.42%, and 34.00%, respectively. The proposed strategy can reduce the frequency fluctuation range and frequency recovery time while maintaining strong adaptability.

INDEX TERMS Adaptive solution method, comprehensive evaluation, load shedding, microgrid, power shortage.

I. INTRODUCTION

As an effective new form of power supply technology that integrates distributed generators (DGs), multi-microgrids (MMGs) can promote local consumption of power from DGs and improve the energy utilization rate [1], [2]. Under constantly changing operation conditions, an MMG can be unintentionally forced to switch to an islanded mode when the utility grids connected to the MMG fail [3]. In this power shortage scenario, output adjustment of the DGs and an underfrequency load shedding (UFLS) strategy are the keys to the safe operation of islanded MMGs [4], [5]. Thus, it is necessary to achieve power balance throgh a UFLS strategy when an islanded MMG suffers a large power shortage.

The associate editor coordinating the review of this manuscript and approving it for publication was Ozan Erdinç.

In recent years, several UFLS strategies have been proposed to address the power shortage problem. In [6], a UFLS strategy based on an implicit enumeration method was proposed. This strategy compensates for the power shortage of an islanded MMG by coordinating the energy storage output and performing load shedding (LS) in an emergency. In [7], a UFLS strategy for islanded microgrids (MGs) was proposed. In this strategy, the probabilities of all scenarios are defined based on a Markov two-state model, and the LS amount and the swing frequency are minimized using a genetic algorithm. In [8], a UFLS method for inverter-based MG was proposed. This method uses frequency variations to estimate power deficits and perform power balancing and frequency recovery through several LS stages. However, this strategy relies on a high-precision physical model and exhibits poor adaptability to changes in the operating state of the MG. To address this limitation, a coordinated LS control scheme based on double Q-learning for an islanded MG was proposed in [9]. In this strategy, the LS action is guided by analyzing information on the MG operating environment. In [10], an improved UFLS method was proposed. This method calculates the power deficit by continuous monitoring of the overshooting signal of the second frequency derivative of the inertia center, and it obtains the optimal load shedding combination through an optimization algorithm to perform frequency recovery. In [11], an undervoltage–frequency LS scheme was proposed. This scheme determines a proper LS amount in an islanded MG by considering the power levels and power factors of various types of loads, such as constant power, constant current, and constant impedance loads. In [12], an effort-based reward approach for the allocation of LS amounts in interconnected MGs was proposed. In this approach, the LS amount is determined based on the effort index, which is defined as the relative contribution of an MG to the network with respect to its capacity. However, the above research has not considered the problem of ensuring a continuous power supply for critical loads when dealing with power shortages. In [13], a local UFLS scheme without real-time communication was proposed. This scheme uses local frequency measurements to estimate the frequency change rate of the inertial center, which is superior to the traditional centralized UFLS scheme in terms of frequency deviation. In [14], a new probability algorithm was adopted to minimize the LS amount at each stage, and a multi-level UFLS scheme based on the frequency response of the wind turbine generator and the uncertainty of the power system was proposed. In [15], a continuous UFLS scheme with precise load control was proposed. This scheme considers the nonlinear factors of frequency threshold and time delay. However, the UFLS schemes in the above works do not have strong adaptability. Therefore, a semi-adaptive multilevel UFLS scheme based on the frequency change rate was proposed in [16]. This scheme can prevent the system frequency from dropping seriously with a low LS amount under the low-inertia scenario caused by the high penetration of renewable power generation. In [17], an adaptive wide-area UFLS scheme was proposed. The amount and locations of LS are determined by the adaptive system frequency response model, which satisfies the dynamic dependence of system load on frequency and voltage deviation. However, the above research does not focus on the evaluation of critical loads. Priority should be given to maintaining a continuous supply for critical loads in an islanded MMG when the system suffers a large power shortage and needs to perform LS. Otherwise, the outage of critical loads will impose large losses on the islanded MMG. Thus, the accurate determination and evaluation of critical loads is an important part of a UFLS strategy.

For the evaluation of critical loads, the application of machine learning methods can yield more objective evaluation results. Meanwhile, machine learning methods can improve the rationality and efficiency of the evaluation process. Neural networks and support vector machines (SVMs) are mainstream machine learning methods, but neural networks are often prone to fall into locally optimal solutions [18], [19]. As a classic tool in machine learning, SVMs can be used to address classification and regression problems. SVMs have unique advantages in processing data with small sample sizes and nonlinear and high-dimensional data sets and are widely used in evaluation models [20], [21]. In [22], a learning scheme that can dynamically predict the stability of the reconnection of subnetworks to the main grid was proposed. This scheme uses an SVM to predict in real-time whether the reconnection of a subnetwork to the main grid would lead to stability or instability. In [23], an islanding detection method was proposed. This method uses an SVM to achieve greater precision in islanding detection and power grid fault detection. Least squares support vector machines (LS-SVMs) are an extension of SVMs. An LS-SVM requires fewer parameters and simplifies the treatment of the problem by converting the inequality constraint of an SVM into an equality constraint. Only a few support vectors determine the final result; therefore, an LS-SVM can focus on evaluating key samples to quickly analyze data and make decisions. This feature endows LS-SVMs with stronger data processing capabilities and high calculation accuracy.

This paper focuses on how to compensate for a large power shortage and maintain a continuous power supply for critical loads within an islanded MMG. Considering the advantages of LS-SVMs, this paper proposes a comprehensive load evaluation method based on a composite least squares support vector machine (CLS-SVM) and a UFLS strategy with an adaptive variation capability. The proposed load evaluation method can account for the various comprehensive evaluation influence factors (CEIFs) of loads and produce reasonable and objective load evaluation results to ensure a continuous power supply for critical loads. The proposed UFLS strategy can quickly compensate for a power shortage and effectively suppress frequency fluctuations during the transition between the grid-connected mode and the islanded mode to achieve power balance and frequency stability.

TABLE 1. Comparison between the first contribution of this paper and the contributions of related literature.

Literature	Consideration of multiple factors of load buses	Comprehensive evaluation of critical loads	Reduction of model calculation complexity	Improvement of result accuracy
[7], [20], [21]			✓	
[8], [10], [11], [12], [13], [17], [22], [23]				✓
[9]			✓	✓
Proposed Strategy	✓	✓	✓	✓

TABLE 2. Comparison between the second contribution of this paper and the contributions of related literature.

Literature	Consideration of load priority	Use of an intelligent algorithm to determine the LS amount and objects	Strong adaptability
[6], [12], [13], [14], [15]		✓	✓
[7], [10], [11]		✓	
[9]	✓	✓	
[13], [16]			✓
Proposed Strategy	✓	✓	✓

The main contributions of this paper can be summarized as follows, and the differences with other studies are shown in Tables 1 and 2:

1) To solve the problem of ensuring a continuous power supply for critical loads, this paper presents a comprehensive load evaluation method based on a CLS-SVM. This proposed method provides a comprehensive evaluation of the load outage loss, loading ratios, load level, and load frequency adjustment effect coefficients (LFAECs). The proposed comprehensive load evaluation method can reduce the influence of isolated points in the load data and improve the accuracy of the load evaluation results.

2) This paper presents a solution method with an adaptive variation capability for the UFLS model. This solution method has a strong global search capability and can quickly obtain the LS results and achieve a power balance by analyzing the load information and constraints.

II. PROBLEM FORMULATION

An islanded MMG loses utility grid power support and relies only on regulating the power output of its DG systems to achieve power balance. When a large power shortage occurs in an islanded MMG after the power output of the DG systems has been adjusted, it is necessary to implement a UFLS strategy to achieve power balance. When the frequency drops, the power shortage can be estimated from the derivative of the frequency [24]:

$$P'_{LS} = \frac{2H_{eq}}{f_N} f'|t \tag{1}$$

where P'_{LS} is the power shortage, f_N is the rated frequency, f is the system frequency, and H_{eq} is the equivalent inertia time constant.

During the power shortage period for an islanded MMG, a change in the power output of the DG systems can cause a change in the power shortage. The power shortage can be updated during the MMG islanding period by means of the following calculation:

$$P_{LS} = P'_{LS} + \frac{2H_{eq}}{f_N} \Delta f'|t \tag{2}$$

where P_{LS} is the updated total power shortage of the islanded MMG.

When a UFLS strategy is implemented, the economy of the MMG should be considered in addition to the LS amount. To optimize the economy of the UFLS strategy, the load operation cost and the load outage loss should also be considered to ensure that the requirements of LS operation are met. The load operation cost and the load outage loss are modeled as follows:

$$C_{c,i} = a_{1,i} \left(P_{LS,i} - P_{LS\max,i}\right)^2 \tag{3}$$

$$C_{n,i} = a_{2,i} P_{LS,i} \tag{4}$$

where $C_{c,i}$ is the operation cost of the ith load, $C_{n,i}$ is the outage loss for the ith load, $a_{1,i}$ is the operation cost coefficient for the ith load, $a_{2,i}$ is the outage loss coefficient for the ith load, $P_{LS,i}$ is the LS amount for the ith load, and $P_{LS\max,i}$ is the maximum LS amount for the ith load.

To reflect the difference in the load outage loss of a single load based on its LS amount, the load outage loss coefficient per LS unit is graded according to the LS amount for a single load. Furthermore, the larger the LS amount is, the larger the outage loss coefficient of the load. The relationship between the outage loss coefficient and the LS amount for a load is shown as follows:

$$a_{2,i} = \begin{cases} a_{21} P_{LS,i} \le P_1 \\ a_{22} P_1 < P_{LS,i} \le P_2 \\ a_{23} P_2 < P_{LS,i} \end{cases} \tag{5}$$

where P_1 is the power threshold between the first and second grades and P_2 is the power threshold between the second and third grades, which satisfy $P_1 < P_2$, and $a_{21} < a_{22} < a_{23}$. Therefore, the load outage loss can be calculated as follows:

$$C_{n,i} = \begin{cases} a_{21} \times P_{LS,i} P_{LS,i} \le P_1 \\ a_{21} \times P_1 + a_{22} \times \left(P_{LS,i} - P_1\right) P_1 < P_{LS,i} \le P_2 \\ a_{21} \times P_1 + a_{22} \times (P_2 - P_1) + a_{23} \times \left(P_{LS,i} - P_2\right) \\ \qquad P_2 < P_{LS,i} \end{cases} \tag{6}$$

In this paper, the objective is to minimize the load operation cost and the load outage loss. The objective function is constructed as follows:

$$\min(\sum_{i=1}^{n} \lambda_i a_{1,i} \left(P_{LS,i} - P_{LS\max,i}\right)^2 + \sum_{i=1}^{n} \lambda_i a_{2,i} P_{LS,i}) \tag{7}$$

where λ_i is the load shedding determination factor (LSDF) value for the ith load.

To meet the requirements of the UFLS strategy, the following constraints should be satisfied:

$$P_{LS,i} \le P_{LS\max,i} \tag{8}$$

$$\sum_{i=1}^{n} P_{LS,i} = P_{LS} \tag{9}$$

$$n_1 \le \sum_{i=1}^{n} \lambda_i \le n_2 \tag{10}$$

$$f_{\min} \le f \le f_{\max} \tag{11}$$

where n_1 and n_2 are the minimum and maximum numbers of loads involved in the UFLS strategy, respectively; f is the bus frequency; and $f_{\min}$ and $f_{\max}$ are the minimum and maximum frequencies of the bus, respectively.

III. COMPREHENSIVE EVALUATION METHOD FOR LOADS BASED ON A CLS-SVM

Achieving a power balance for an islanded MMG and maintaining a continuous power supply for critical loads are the key research contents addressed in this section. Factors such as loading ratios, load outage losses, and load levels can affect the determination of critical loads. To select LS objects more reasonably and objectively to ensure a continuous supply for critical loads, the proposed comprehensive load evaluation method relies on fuzzy mathematics to determine the membership degrees of the CEIFs. The evaluation grades of the load CEIFs are obtained based on the membership degrees of the load CEIFs. Considering the evaluation grades of the load CEIFs can reduce the deviations in the accuracy of model training caused by isolated points in the data. Then, an LS-SVM is used to determine the LSDFs based on the evaluation grades of the CEIFs. Finally, the problem of determining critical loads is transformed into a typical 0-1 planning problem, in which the 0-1 variables describe the determination of critical loads and alternative shedding loads.

A. EVALUATION GRADE DETERMINATION FOR LOAD CEIFs

Some fuzziness will arise in the process of evaluating critical loads when a certain CEIF of the loads changes from one characteristic to another, such as when the influence degree changes from large to small. This fuzziness increases the challenge of judging the influence degrees. Fuzzy mathematics can be used to handle such fuzziness by applying exact mathematics to objective objects. As the core of a fuzzy set, the membership degree function has an important significance in fuzzy mathematics [25], [26]. Corresponding membership degree functions should be chosen to describe different types of fuzzy concepts. The steps of determining the evaluation grades for the load CEIFs are as follows:

1) The data set is constructed. To obtain the fuzzy membership degrees of the load CEIFs, a data set

is constructed in this paper based on the load data.

$$X = \begin{bmatrix} X_1 \\ X_2 \\ \vdots \\ X_n \end{bmatrix} = \begin{bmatrix} L_1 & F_1 & D_1 & R_1 \\ L_2 & F_2 & D_2 & R_2 \\ \vdots & \vdots & \vdots & \vdots \\ L_n & F_n & D_n & R_n \end{bmatrix} \tag{12}$$

where X_i is a matrix consisting of data regarding the CEIFs of the loads, L_i is the outage loss of the ith load, F_i is the loading ratio of the ith load, D_i is the load level of the ith load, and R_i is the LFAEC of the ith load.

2) The evaluation set of CEIFs is constructed. The evaluation set contains all possible evaluation results for the CEIFs. The evaluation set is expressed as $V = \{v_1, v_2, \cdots, v_n\}$, where v_i indicates the evaluation grade and the degree of influence of the ith CEIF. For the determination of v_i, values of $V = \{1, 2, 3, 4, 5\}$ are considered in this paper. The higher the grade is, the larger the influence degree.

3) The membership degree function for each evaluation grade is determined. The membership degree function can be used to perform dimensionless processing on variables. For the fuzzy processing of the data, a trapezoidal membership degree function is selected in this paper based on the evaluation grade set and the consideration of computational convenience.

$$A_i(x) = \begin{cases} 0 & x \le a \\ \dfrac{x-a}{b-a} & a < x \le b \\ 1 & b < x \le c \\ \dfrac{d-x}{d-c} & c < x \le d \\ 0 & d < x \end{cases} \tag{13}$$

where $a \le b \le c \le d$.

4) The membership degrees of the data are determined based on the membership degree functions. The determination of the fuzzy membership degrees for the ith CEIF is shown in Fig. 1. First, the entire numerical space is divided into 5 numerical ranges in accordance with the evaluation grade set. These 5 numerical ranges are $\{x_1, x_3, x_2, x_5, x_4, x_7, x_6, x_9, x_8, x_{10}\}$, where x_1 and x_{10} are

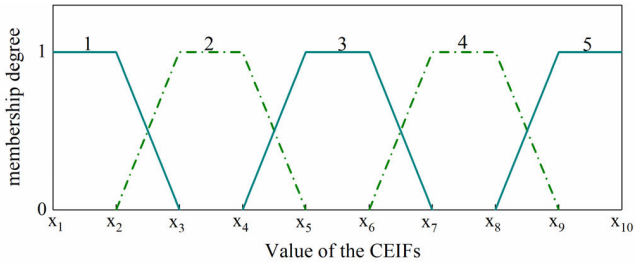

FIGURE 1. Fuzzy membership degree function for each evaluation grade.

the minimum and maximum values, respectively, of the ith CEIF. Then the CEIF data are substituted into the membership degree function for each evaluation grade to obtain the corresponding membership degree. The fuzzy membership degrees based on each evaluation grade are expressed as $U = \{u_1, u_2, u_3, u_4, u_5\}$, where $u_i \in [0, 1]$.

5) The evaluation result set for the load CEIFs is constructed. The evaluation grade v_i is determined in accordance with the principle of the maximum membership degree based on U as calculated in step 4. Then, the evaluation grade set x of the loads and the evaluation grade set x_i of the ith load are constructed based on v_i.

$$x = \begin{bmatrix} x_1 \\ x_2 \\ \vdots \\ x_n \end{bmatrix} = \begin{bmatrix} l_1\ f_1\ d_1\ r_1 \\ l_2\ f_2\ d_2\ r_2 \\ \vdots\ \vdots\ \vdots\ \vdots \\ l_n\ f_n\ d_n\ r_n \end{bmatrix} \tag{14}$$

where l_i is the outage loss evaluation grade of the ith load, f_i is the loading ratio evaluation grade of the ith load, d_i is the load level evaluation grade of the ith load, and r_i is the LFAEC of the ith load.

The determination of the evaluation grade set for each CEIF makes the CEIFs of different attributes comparable. Furthermore, the results are more accurate when this load evaluation method is used.

B. DETERMINATION OF THE LOAD EVALUATION RESULTS BASED ON AN LS-SVM

As a machine learning method based on data mining, an LS-SVM is a learning machine that achieves an improved generalization ability by seeking to minimize structured risk. In the case of a small sample size, an LS-SVM can also achieve better evaluation results than other similar models [27]. Considering the aforementioned advantages of LS-SVMs, this paper presents a load evaluation method based on a CLS-SVM. This method obtains a load evaluation function through training on a sample set of loads. The architecture of the CLS-SVM used in the proposed load evaluation method is shown in Fig. 2. The process flow of the determination of the load evaluation results based on a CLS-SVM is shown in Fig. 3. The detailed steps are as follows:

1) The sample set of loads, $S = (x_j, \lambda_j)(j = 1, 2, \cdots, n)$, is built, where the samples x_j are obtained using the previously described process for determining the evaluation grades of the load CEIFs. $x_j = [l_j, f_j, d_j, r_j]$ is the d-dimensional input, and λ_j is the LSDF value of the sample set.

2) The optimal hyperplane is determined. The determination of the optimal hyperplane is an important step of the evaluation method. The load CEIFs constitute multidimensional input, so a nonlinear transformation kernel function $\varphi(x)$ needs to be introduced to map this multidimensional input from the original space to a high-dimensional feature space before determining the optimal hyperplane. The process of kernel function feature mapping is illustrated in Fig. 4. Then the optimal load hyperplane is constructed in the high-dimensional feature space and expressed as follows:

$$f(x) = \omega^T \varphi(x) + b_2 \tag{15}$$

The optimization problem is

$$\min \frac{1}{2}\omega^T \omega + \frac{1}{2} c_1 \sum_{i=1}^{N} \xi^2 \tag{16}$$

subject to

$$y_i = \omega^T \varphi(x_i) + b_2 + \xi \ i = 1, \ldots, n \tag{17}$$

where ω is the normal vector of the hyperplane, b_2 is the parameter to be determined, ξ is the difference between the actual output and the predicted output, and c_1 is an adjustment parameter.

3) The load evaluation function is determined. A Lagrangian function is introduced to address the optimization problem in step 2. The load evaluation function for an LS-SVM can be expressed as follows:

$$y(x) = \sum_{i=1}^{n} a_i K(x, x_i) + b_2 \tag{18}$$

where a_i is a Lagrange multiplier and $K(x_i, x_j) = \langle \varphi(x_i), \varphi(x_j) \rangle$.

4) The load evaluation results are obtained by solving the load evaluation function based on the load data. Based on the function values, the LSDFs are obtained; then, the comprehensive evaluation of the critical loads is completed, and the corresponding LS positions are determined.

IV. SOLUTION METHOD FOR THE UFLS MODEL

When solving a UFLS model, the existing algorithms tend to fall into local optima [28]. Different from particle swarm optimization (PSO), the grasshopper optimization algorithm (GOA) is a group-based nature-inspired calculation method. The updating of the search agent positions is affected by the position of each search agent, allowing the GOA to effectively achieve gradual and balanced exploration of the search space when searching for the optimal results [29], [30]. Therefore, the GOA is a suitable method for solving the proposed UFLS model.

The global and local exploitation capabilities of the GOA are coordinated in each iteration by means of a decreasing coefficient. However, because this decreasing coefficient

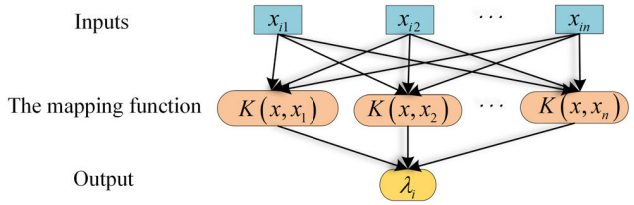

FIGURE 2. CLS-SVM architecture.

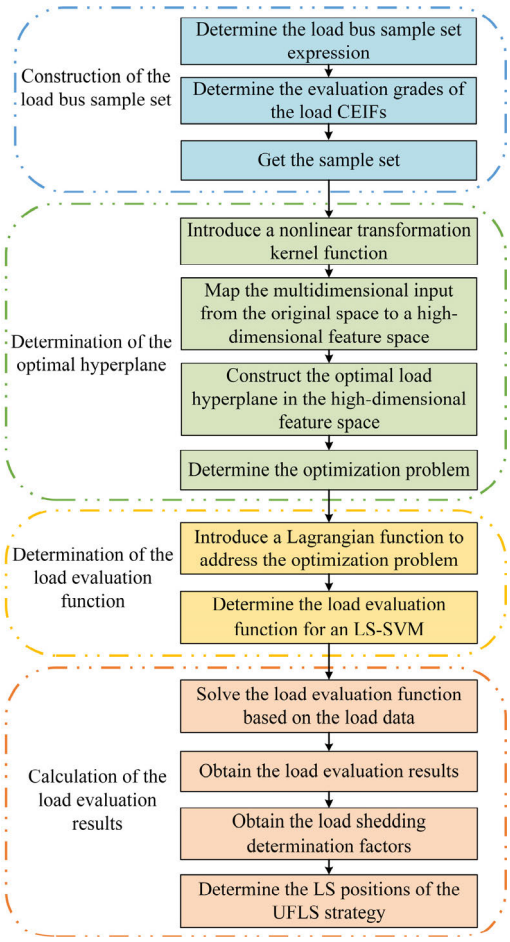

FIGURE 3. The process flow of the determination of the load evaluation results based on the CLS-SVM.

decreases linearly as the number of iterations increases, the convergence speed of the GOA is poor. Therefore, based on the GOA, this paper proposes a solution method with an adaptive variation capability for solving the proposed UFLS model. The proposed solution method uses a nonlinearly decreasing coefficient instead of the original linearly decreasing coefficient. Thus, the proposed solution method achieves a better global search capability and improved self-adaptability.

For solving the UFLS model, the flow chart of the proposed solution method is shown in Fig. 5. The detailed steps of the proposed solution method are as follows:

Step 1: The parameters used in the solution method are initialized, including power and LS constraints for each load.

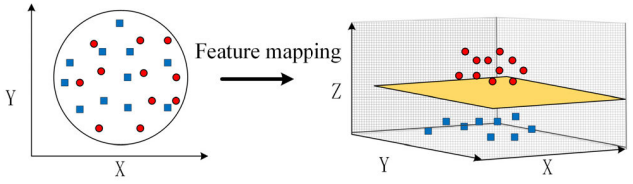

FIGURE 4. Kernel function feature mapping.

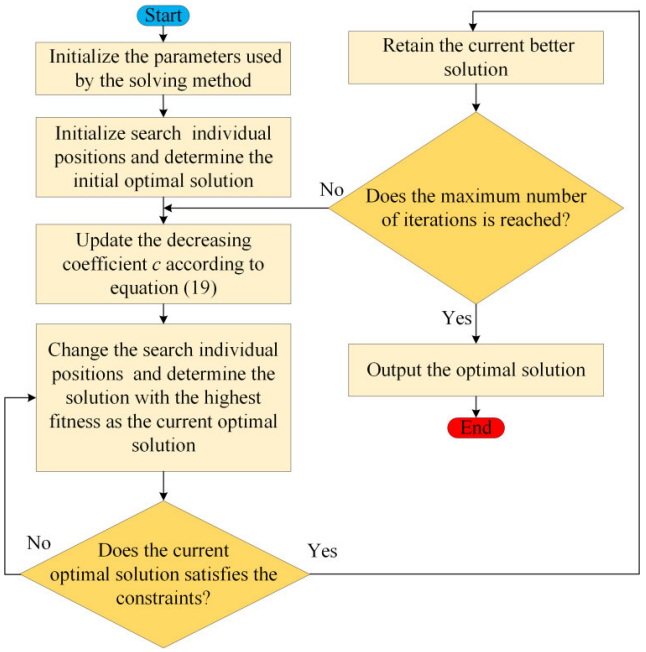

FIGURE 5. Process flow of the proposed solution method.

Step 2: The individual search positions are initialized, the fitness values of all initial solutions are calculated, and the solution with the highest fitness is retained as the initial optimal solution.

Step 3: The nonlinearly decreasing coefficient c is updated based on the following equation:

$$c = a \times \left[\cos\left(\frac{(l-1)\pi}{L}\right) + 1\right] \times \left(c_{\max} - l \times \frac{c_{\max} - c_{\min}}{L}\right) \tag{19}$$

where c is the decreasing coefficient, l is the current iteration, and L is the maximum number of iterations. In this paper, $c_{\max} = 1$ and $c_{\min} = 0.00001$.

Step 4: The individual search positions are modified, the fitness of the values of the current solutions is updated based on equation (20), and the solution with the highest fitness is retained as the current optimal solution.

$$X_i^d = c\left(\sum_{\substack{j=l \\ j \neq i}}^{N} c\frac{ub_d - lb_d}{2} s\left(\left|x_j^d - x_i^d\right|\right)\frac{x_i - x_j}{d_{ij}}\right) + T_d{}^{\Lambda} \tag{20}$$

where ub_d and lb_d are the upper and lower bounds, respectively, of the d-dimensional search space and $T_d{}^{\Lambda}$ is the optimal value in the current population.

Step 5: If the current optimal solution satisfies the constraints, this solution is retained. Otherwise, the algorithm returns to Step 4.

Step 6: The objective function value of the current optimal solution is compared against that of the previous optimal solution, and the optimal solution with the smaller objective function value is retained.

Step 7: If the maximum number of iterations has been reached, the optimal LS results are output. Otherwise, the algorithm returns to Step 3 to continue the search for the optimal solution.

V. RESULTS

A. PERFORMANCE VERIFICATION OF THE PROPOSED LOAD EVALUATION METHOD

To verify that the load evaluation method based on a CLS-SVM that is proposed in this paper can be effectively applied to carry out sample training and perform a correct evaluation analysis, the data of 40 load samples were fuzzified, and the obtained evaluation results were substituted into the sample data. Of the 40 load samples, 30 were selected as the training samples, among which the numbers of samples belonging to categories 0 and 1 were 14 and 16, respectively, and the remaining 10 load samples were selected as the prediction samples. To enhance the evaluation accuracy, the radial basis function (RBF) kernel function was selected, and the kernel function parameters were determined through cross-validation. First, 5 load samples from each category were randomly selected as prediction samples, and the remaining samples were used as training samples. Then, the proposed comprehensive load evaluation method based on a CLS-SVM was trained.

As shown in Fig. 6 and Table 3, the evaluation accuracy rates of the proposed CLS-SVM method in 5 random training iterations were 100%, 90%, 90%, 100%, and 80%. The average evaluation accuracy rate was 92%. As shown in Fig. 7 and Table 3, the evaluation accuracy rates of an evaluation method based on an LS-SVM were only 80%, 70%, 80%, 70%, and 80% under the same random training conditions. With this method, the average accuracy rate was only 76%. This is because the CLS-SVM is less dependent on parameters; the treatment of the problem can therefore be simplified by converting the inequality constraint of the SVM into an equality constraint. At the same time, this method can reduce the impact of isolated points in the load bus data on the evaluation results, and it can focus on assessing key samples to quickly analyze data and make decisions, thus improving the data processing capacity and the accuracy of the load evaluation results. These findings verify that the proposed evaluation method based on a CLS-SVM exhibits high accuracy when the data are later fuzzified under random conditions.

B. FEASIBILITY ANALYSIS OF THE UFLS STRATEGY IN THE ISLANDING SCENARIO

To verify the effectiveness of the proposed UFLS strategy, a modified IEEE 33-bus system model was built in the

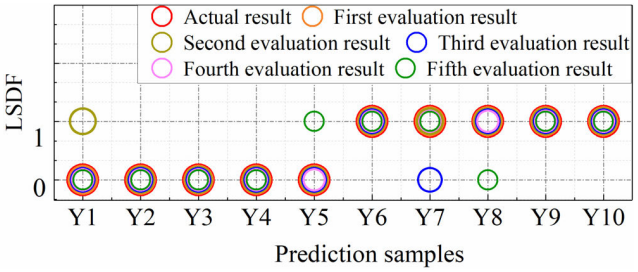

FIGURE 6. Results of the proposed evaluation method based on a CLS-SVM.

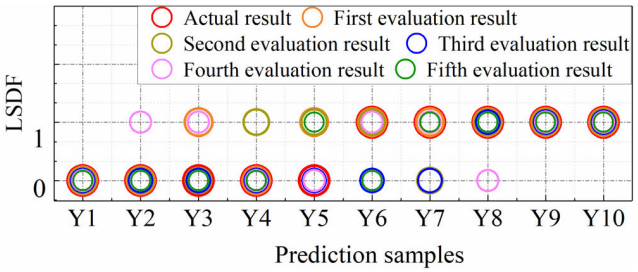

FIGURE 7. Results of an evaluation method based on an LS-SVM.

MATLAB/SIMULINK platform. All the simulations in this paper are based on MATLAB R2016a/Simulink software and were performed on a computer equipped with an Intel (R) Core (TM) i5. The processor operates at 2.90 GHz with 16 GB of RAM. As shown in Fig. 8, this model contains seven battery energy storage units (BESs), and BES1 in MG-1 is selected as the primary BES and enters the V/f control mode when islanding occurs. The rest of the BESs and eight photovoltaic units (PVs) operate in the PQ control mode. The data information for the 9 loads in this model is shown in Table 4. The power information of the DGs, loads, and BESs in the MMG is shown in Table 5. The model parameter information is shown in Table 6. A reference to the load data of the system model is provided in [31].

The MMG system enters the islanded mode at t=1.2 s. At this time, the DGs need to increase their active power output after the occurrence of the islanding event to compensate for the power shortage caused by the unintentional islanding transition. The original tie-line power is 260 kW. When a power balance within the islanded MMG cannot be satisfied even after adjusting the DG outputs, it is necessary to shed part of the loads. During the execution of the UFLS strategy, the communication transmission delay time is set to 10 ms, and the relay start delay and the LS delay are set to 10 ms [32].

1) CONTROL PERFORMANCE ANALYSIS OF DIFFERENT UFLS STRATEGIES

The required LS amount is calculated as 183 kW via equation (2) based on the measured frequency. The shedding situations based on different UFLS strategies are shown in Fig. 9. UFLS strategy 2 is a UFLS strategy that considers only the load level [8], and UFLS strategy 3 is a UFLS strategy based on an intelligent algorithm [10].

TABLE 3. Comparison of the evaluation accuracy rates of different evaluation methods.

Number of comparisons	Accuracy rate of the evaluation method based on LS-SVM	Accuracy rate of the proposed evaluation method based on CLS-SVM
1	80%	100%
2	70%	90%
3	80%	90%
4	70%	100%
5	80%	80%
Average accuracy	76%	92%

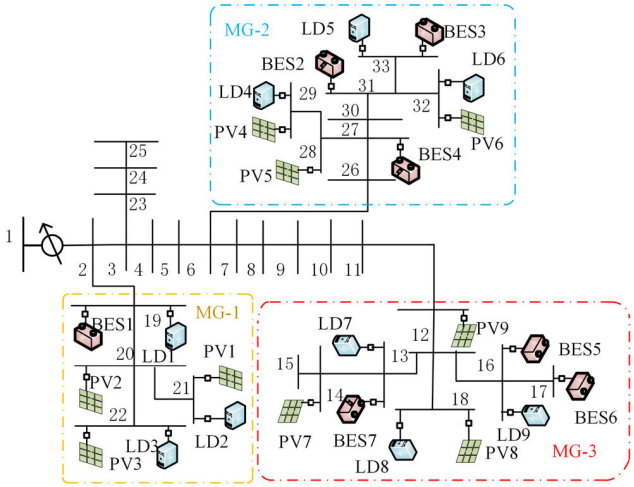

FIGURE 8. MMG model based on a modified IEEE 33-bus system.

TABLE 4. System load data information.

Load number	l	f	d	r	P/kW
LD1	4	3	1	2	80
LD2	2	3	3	1	60
LD3	5	4	5	2	50
LD4	1	4	4	3	70
LD5	3	5	5	5	50
LD6	2	2	2	3	60
LD7	4	5	3	4	40
LD8	3	4	4	3	60
LD9	1	1	3	3	80

TABLE 5. Configuration information for the MMG.

Microgrid	MG1	MG1	MG1
Rated PV power (kW)	30,30,30	30,30,30	30,30,30
Total (kW)	90	90	90
Rated BES power (kW)	95	10,10,10	10,10,10
BES output power before islanding (kW)	10	10,10,10	10,10,10
Rated load capacity (kW)	80,60,50	70,50,60	40,60,80
Total (kW)	190	180	180

Based on the proposed load evaluation method, the loads are evaluated comprehensively and shed in accordance with the evaluation results. The LS situations of each load under different UFLS strategies are shown in Fig. 9. During the power shortage period, the proposed UFLS method comprehensively analyzes the situation of each load to find the optimal solution in terms of the objective function. As shown in Fig. 9 (a), part of the loads are shed from LD1, LD2, LD4, LD6, and LD9 under the premise of satisfying the LS constraints. UFLS strategy 2 considers only the load level during the LS period and sorts the loads from low to high according to their load levels. As shown in Fig. 9 (b), all the loads are shed in LD1 and LD6, and the loads are partially shed in LD8, which causes an outage of power to the critical load LD8. As shown in Fig. 9 (c), under UFLS strategy 3, partial LS is performed in LD1, LD2, LD3, LD4, LD5, LD6, LD7, LD8 and LD9. This LS situation results in power outages to the critical loads LD3, LD5, LD7, and LD8. These power outages to critical loads occur mainly because this UFLS strategy does not include a comprehensive evaluation of the loads.

TABLE 6. The model parameter information.

Parameter	Value
The rated frequency of the bus f_N	50 Hz
The minimum frequency of the bus $f_{\min}$	49.5 Hz
The maximum frequency of the bus $f_{\max}$	50.5 Hz
The operating cost coefficient corresponding to the load level $a_{1,i}$ ($i=1,2,K,5$)	0.13\$/kWh, 0.29\$/kWh, 0.57\$/kWh, 0.88\$/kWh, 0.96\$/kWh
The LS determination factor value corresponding to the load level λ_i ($i=1,2,K,5$)	0.24, 0.37, 0.55, 0.71, 0.83
The outage loss coefficients of unit load a_{21} , a_{22} , a_{23}	1.26\$/kWh, 2.46\$/kWh, 3.03\$/kWh

The frequency curves corresponding to the three UFLS strategies are shown in Fig. 10. Loads with high load levels should be retained, and loads with low load levels should be shed first during the LS period. The LFAECs during the LS period are another important factor to consider. The proposed strategy integrates the load levels and the LFAECs. The selection of LS objects tends more toward loads with low load levels and LFAECs when the proposed UFLS strategy is implemented. This selection approach can effectively slow down the frequency drop and quickly restore the frequency to the rated value. LD1, LD2, LD4, LD6, and LD9 are selected under the proposed UFLS strategy, and the selection of these LS objects results in a small frequency fluctuation range and a short frequency recovery time. The range of the frequency fluctuations during the islanding period is 49.41–50.25 Hz. The frequency is restored to a steady state after 0.2 s. In contrast, the frequency fluctuates over a large range during the islanding period under UFLS strategy 2 and UFLS strategy 3. The minimum frequency fluctuation under UFLS strategy 2 is 49.24 Hz, the maximum frequency fluctuation under UFLS strategy 3 is 50.30 Hz, and the frequency takes a long time

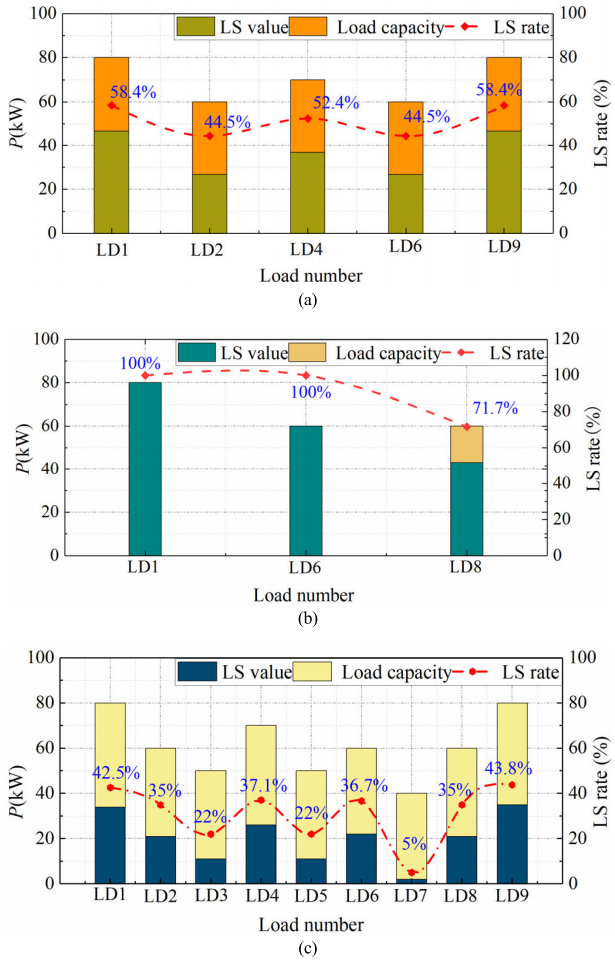

FIGURE 9. LS situations of each load under three UFLS strategies. (a) LS situation of each load under the proposed UFLS strategy. (b) LS situation of each load under UFLS strategy 2. (c) LS situation of each load under UFLS strategy 3.

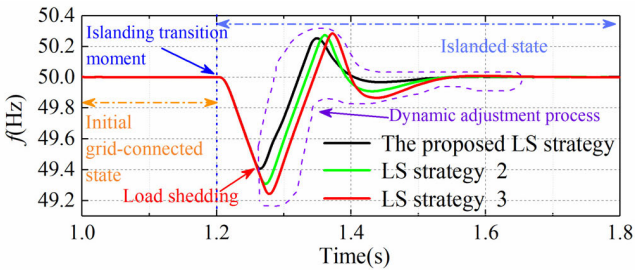

FIGURE 10. MMG frequency waveforms under three UFLS strategies.

to return to a steady-state. The aforementioned results show that the proposed UFLS strategy can effectively eliminate power shortages during the islanding period. Furthermore, the proposed UFLS strategy can reduce the frequency fluctuation range and quickly restore the frequency to a stable state.

2) ADAPTIVITY ANALYSIS OF SOLUTION METHODS FOR THE UFLS MODEL

As a solution method iterates to find the optimal solution, a coefficient with a larger value in the early stage can help the

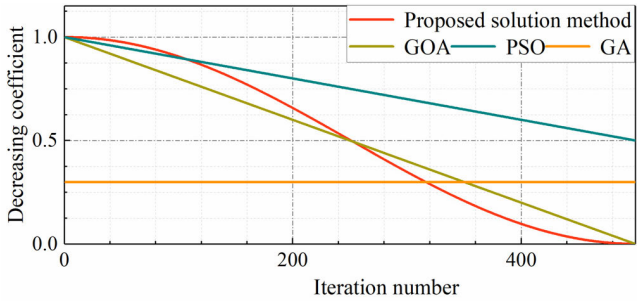

FIGURE 11. Variation in the decreasing coefficient under four solution methods.

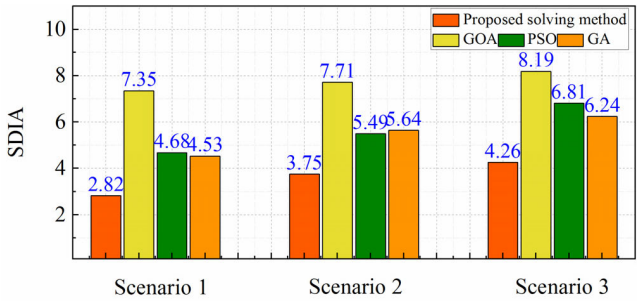

FIGURE 12. SDIAs of four solution methods in 3 scenarios.

solution method perform an effective global search, while a coefficient with a smaller value in the later stage can help the solution method search locally and converge to an optimal solution quickly. In this section, the solution performances of the GOA, PSO, a genetic algorithm (GA), and the proposed solution method are compared and analyzed. The variation in the decreasing coefficient under each of the four solution methods is shown in Fig. 11. In the proposed solution method, the decreasing coefficient is nonlinearly varying. Compared with the linearly decreasing coefficients of the GOA, PSO, and the GA, the decreasing coefficient of the proposed solution method takes larger values in early iterations and smaller values in later iterations. The nonlinear variation in the decreasing coefficient of the proposed solution method allows it to better meets the requirements of an effective solution method.

For this analysis, the performance of PSO, the GOA, the GA, and the proposed solution method was tested in 3 scenarios based on solving the UFLS model. As shown in Fig. 12, Scenarios 1, 2, and 3 correspond to the standard deviations of the iterative average (SDIAs) calculated 50, 100, and 150 times, respectively, using each of the four solution methods. The standard deviation is a quantitative metric that reflects the degree of dispersion of a data set and is an important indicator of accuracy. In Scenario 1, the SDIA of the proposed solution method is significantly smaller than those of PSO, the GOA, and the GA. In Scenarios 2 and 3, although the SDIAs of the proposed solution method slightly increase compared with Scenario 1, their values are still smaller than those of PSO, the GOA, and the GA. The better SDIA performance of the proposed solution method shows

that this method is more adaptive than the methods considered for comparison and has better convergence stability.

VI. DISCUSSION

To achieve power balance and analyze the comprehensive effects of loads in an islanded MMG, this paper proposes a UFLS strategy based on a CLS-SVM. This UFLS strategy integrates multiple CEIFs of loads so that the load evaluation method does not unilaterally rely on a particular index. This feature of the proposed UFLS strategy improves the objectivity of the comprehensive evaluation method and reduces the influence of isolated points in the CEIFs on the evaluation accuracy. For solving the UFLS model, a solution method with improved adaptability and accuracy is proposed. The feasibility of the proposed LS strategy is verified in the scenario of a large power shortage in an islanded MMG. The results show that the proposed UFLS strategy can eliminate power shortages in islanded MMGs and reduce the frequency fluctuation range and frequency recovery time compared with two other compared UFLS strategies. Furthermore, the proposed UFLS strategy improves the operational stability of the islanded MMG while ensuring the supply reliability for critical loads.

REFERENCES

[1] C. Reiz and J. B. Leite, "Optimal coordination of protection devices in distribution networks with distributed energy resources and microgrids," *IEEE Access*, vol. 10, pp. 99584–99594, 2022.

[2] B. Zhu, Y. Liu, S. Zhi, K. Wang, and J. Liu, "A family of bipolar high step-up zeta–buck–boost converter based on 'coat circui,'" *IEEE Trans. Power Electron.*, vol. 38, no. 3, pp. 3328–3339, Mar. 2023.

[3] M. Tofighi-Milani, S. Fattaheian-Dehkordi, M. Gholami, M. Fotuhi-Firuzabad, and M. Lehtonen, "A novel distributed paradigm for energy scheduling of islanded multiagent microgrids," *IEEE Access*, vol. 10, pp. 83636–83649, 2022.

[4] C. Wang, S. Mei, Q. Dong, R. Chen, and B. Zhu, "Coordinated load shedding control scheme for recovering frequency in islanded microgrids," *IEEE Access*, vol. 8, pp. 215388–215398, 2020.

[5] C. Wang, S. Chu, Y. Ying, A. Wang, R. Chen, H. Xu, and B. Zhu, "Underfrequency load shedding scheme for islanded microgrids considering objective and subjective weight of loads," *IEEE Trans. Smart Grid*, early access, Aug. 31, 2022, doi: 10.1109/TSG.2022.3203172.

[6] C. Wang, X. Li, T. Tian, Z. Xu, and R. Chen, "Coordinated control of passive transition from grid-connected to islanded operation for three/single-phase hybrid multimicrogrids considering speed and smoothness," *IEEE Trans. Ind. Electron.*, vol. 67, no. 3, pp. 1921–1931, Mar. 2020.

[7] Y.-Y. Hong, M.-C. Hsiao, Y.-R. Chang, Y.-D. Lee, and H.-C. Huang, "Multiscenario underfrequency load shedding in a microgrid consisting of intermittent renewables," *IEEE Trans. Power Del.*, vol. 28, no. 3, pp. 1610–1617, Jul. 2013.

[8] E. Dehghanpour, H. K. Karegar, and R. Kheirollahi, "Under frequency load shedding in inverter based microgrids by using droop characteristic," *IEEE Trans. Power Del.*, vol. 36, no. 2, pp. 1097–1106, Apr. 2021.

[9] C. Wang, S. Chu, H. Yu, Y. Ying, and R. Chen, "Control strategy of unintentional islanding transition with high adaptability for three/single-phase hybrid multimicrogrids," *Int. J. Electr. Power Energy Syst.*, vol. 136, Mar. 2022, Art. no. 107724.

[10] J. Jallad, S. Mekhilef, J. A. Laghari, and H. Mokhlis, "Improved UFLS with consideration of power deficit during shedding process and flexible load selection," *IET Renew. Power Gener.*, vol. 12, no. 5, pp. 565–575, 2018.

[11] S. Rahmani, A. Rezaei-Zare, M. Rezaei-Zare, and A. Hooshyar, "Voltage and frequency recovery in an islanded inverter-based microgrid considering load type and power factor," *IEEE Trans. Smart Grid*, vol. 10, no. 6, pp. 6237–6247, Nov. 2019.

[12] A. Hussain, V. Bui, and H. Kim, "An effort-based reward approach for allocating load shedding amount in networked microgrids using multiagent system," *IEEE Trans. Ind. Informat.*, vol. 16, no. 4, pp. 2268–2279, Apr. 2020.

[13] M. Sun, G. Liu, M. Popov, V. Terzija, and S. Azizi, "Underfrequency load shedding using locally estimated RoCoF of the center of inertia," *IEEE Trans. Power Syst.*, vol. 36, no. 5, pp. 4212–4222, Sep. 2021.

[14] A. A. Zadeh, A. Sheikhi, and W. Sun, "A novel probabilistic method for under frequency load shedding setting considering wind turbine response," *IEEE Trans. Power Del.*, vol. 37, no. 4, pp. 2640–2649, Aug. 2022.

[15] C. Li, Y. Wu, Y. Sun, H. Zhang, Y. Liu, Y. Liu, and V. Terzija, "Continuous under-frequency load shedding scheme for power system adaptive frequency control," *IEEE Trans. Power Syst.*, vol. 35, no. 2, pp. 950–961, Mar. 2020.

[16] S. S. Banijamali and T. Amraee, "Semi-adaptive setting of under frequency load shedding relays considering credible generation outage scenarios," *IEEE Trans. Power Del.*, vol. 34, no. 3, pp. 1098–1108, Jun. 2019.

[17] T. Shekari, F. Aminifar, and M. Sanaye-Pasand, "An analytical adaptive load shedding scheme against severe combinational disturbances," *IEEE Trans. Power Syst.*, vol. 31, no. 5, pp. 4135–4143, Sep. 2016.

[18] L. Xi, J. Wu, Y. Xu, and H. Sun, "Automatic generation control based on multiple neural networks with actor-critic strategy," *IEEE Trans. Neural Netw. Learn. Syst.*, vol. 32, no. 6, pp. 2483–2493, Jun. 2021.

[19] R. M. Balabin, E. I. Lomakina, and R. Z. Safieva, "Neural network (ANN) approach to biodiesel analysis: Analysis of biodiesel density, kinematic viscosity, methanol and water contents using near infrared (NIR) spectroscopy," *Fuel*, vol. 90, no. 5, pp. 2007–2015, May 2011.

[20] W. Zhao, J. Zhang, and K. Li, "An efficient LS-SVM-based method for fuzzy system construction," *IEEE Trans. Fuzzy Syst.*, vol. 23, no. 3, pp. 627–643, Jun. 2015.

[21] Z. S. Hosseini, M. Mahoor, and A. Khodaei, "AMI-enabled distribution network line outage identification via multi-label SVM," *IEEE Trans. Smart Grid*, vol. 9, no. 5, pp. 5470–5472, Sep. 2018.

[22] C. Lassetter, E. Cotilla-Sanchez, and J. Kim, "A learning scheme for microgrid reconnection," *IEEE Trans. Power Syst.*, vol. 33, no. 1, pp. 691–700, Jan. 2018.

[23] H. R. Baghaee, D. Mlakic, S. Nikolovski, and T. Dragicevic, "Support vector machine-based islanding and grid fault detection in active distribution networks," *IEEE J. Emerg. Sel. Topics Power Electron.*, vol. 8, no. 3, pp. 2385–2403, Sep. 2020.

[24] A. Ketabi and M. H. Fini, "An underfrequency load shedding scheme for islanded microgrids," *Int. J. Electr. Power Energy Syst.*, vol. 62, pp. 599–607, Nov. 2014.

[25] W.-B. Xie, S. Sang, H.-K. Lam, and J. Zhang, "A polynomial membership function approach for stability analysis of fuzzy systems," *IEEE Trans. Fuzzy Syst.*, vol. 29, no. 8, pp. 2077–2087, Aug. 2021.

[26] C. Wang, S. Mei, H. Yu, S. Cheng, L. Du, and P. Yang, "Unintentional islanding transition control strategy for three-/single-phase multimicrogrids based on artificial emotional reinforcement learning," *IEEE Syst. J.*, vol. 15, no. 4, pp. 5465–5475, Dec. 2021.

[27] S. Yin, Y. Jiang, Y. Tian, and O. Kaynak, "A data-driven fuzzy information granulation approach for freight volume forecasting," *IEEE Trans. Ind. Electron.*, vol. 64, no. 2, pp. 1447–1456, Feb. 2017.

[28] C. Wang, Q. Dong, S. Mei, X. Li, S. Kang, and H. Wang, "Seamless transition control strategy for three/single-phase multimicrogrids during unintentional islanding scenarios," *Int. J. Electr. Power Energy Syst.*, vol. 133, Dec. 2021, Art. no. 107257.

[29] P. Qin, H. Hu, and Z. Yang, "The improved grasshopper optimization algorithm and its applications," *Sci. Rep.*, vol. 11, no. 1, p. 23733, Dec. 2021.

[30] R. Purushothaman, S. P. Rajagopalan, and G. Dhandapani, "Hybridizing gray wolf optimization (GWO) with grasshopper optimization algorithm (GOA) for text feature selection and clustering," *Appl. Soft Comput.*, vol. 96, Nov. 2020, Art. no. 106651.

[31] S. Gao, S. Liu, Y. Liu, X. Zhao, and T. E. Song, "Flexible and economic dispatching of AC/DC distribution networks considering uncertainty of wind power," *IEEE Access*, vol. 7, pp. 100051–100065, 2019.

[32] C. Wang, H. Yu, L. Chai, H. Liu, and B. Zhu, "Emergency load shedding strategy for microgrids based on dueling deep Q-learning," *IEEE Access*, vol. 9, pp. 19707–19715, 2021.

RAN CHEN received the M.S. degree in electrical engineering from the Wuhan University of Technology, Wuhan, China, in 2013. He is currently a Senior Engineer with the State Grid Hubei Economic Research Institute. His current research interests include microgrid operation and coordinated control and digital control of substations.

HANPING XU is currently a Professor-Level Senior Engineer with the State Grid Hubei Economic Research Institute. His current research interests include digital control of substations and microgrid energy management.

LI ZHOU is currently a Senior Engineer with the State Grid Hubei Economic Research Institute. His current research interests include operation optimization of smart grids and digital control of substations.

JIE CAI is currently a Senior Engineer with the State Grid Hubei Economic Research Institute. His current research interests include microgrid energy management and digital control of substations.

CHUANYU XIONG is currently an Engineer with the State Grid Hubei Economic Research Institute. His current research interests include microgrid operation and control and digital control of substations.

YINGBO ZHOU received the Ph.D. degree in geotechnical engineering from the Institute of Rock and Soil Mechanics, Chinese Academy of Sciences, in 2016. He is currently a Senior Engineer with the State Grid Hubei Economic Research Institute. His current research interests include power engineering disaster prevention and mitigation.

XUEFEI ZHANG was born in Hubei, China. She is currently pursuing the M.S. degree in electrical engineering with China Three Gorges University, Yichang, China. Her research interests include distributed generation and operation optimization of smart grids.

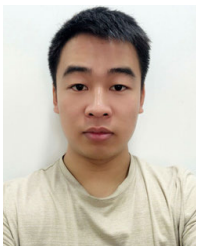

QINGGUO DONG was born in Henan, China. He is currently with State Grid Heze Power Supply Company. His research interests include distributed generation and microgrid operation and control.

CAN WANG (Member, IEEE) was born in Hubei, China. He received the Ph.D. degree in electrical engineering from the South China University of Technology, Guangzhou, China, in 2017.

He is currently an Associate Professor in electrical engineering with the College of Electrical Engineering and New Energy, China Three Gorges University, Yichang, China. His current research interests include distributed generation, microgrid operation and control, integrated energy systems, and smart grids. He served as the Co-Chair for the Special Session on "Power Systems with Penetration of RE and EV" in IEEE IGBSG 2019. He is a member of the Youth Editorial Committee of Electric Power. He is an Active Reviewer of IEEE TRANSACTIONS ON SUSTAINABLE ENERGY, IEEE TRANSACTIONS ON INDUSTRIAL ELECTRONICS, IEEE SYSTEMS JOURNAL, *IET Power Electronics*, *IET Renewable Power Generation*, and IEEE ACCESS.

NAN YANG (Senior Member, IEEE) received the B.S. degree in electrical engineering from the Taiyuan University of Technology, Taiyuan, China, in 2009, and the Ph.D. degree in electrical engineering from Wuhan University, Wuhan, China, in 2014. He is currently an Associate Professor with the College of Electrical Engineering and New Energy, China Three Gorges University, Yichang, China. His major research interests include power dispatching automation of new energy sources, artificial intelligence, planning and operation of power systems, operation and control of microgrid, and active distribution networks.